Elimination of the Fast Transient in Superior Cervical Ganglion Neurons with Expression of KV4.2W362F: Molecular Dissection of I_A

Sacha A. Malin and Jeanne M. Nerbonne

Department of Molecular Biology and Pharmacology, Washington University School of Medicine, St. Louis, Missouri 63110

Electrophysiological and molecular studies have revealed considerable heterogeneity in voltage-gated K^+ currents and in the subunits that underlie these channels in mammalian neurons. At present, however, the relationship between native K^+ currents and cloned subunits is poorly understood. In the experiments here, a molecular genetic approach was exploited to define the molecular correlate of the fast transient outward K^+ current, I_{Af}, in sympathetic neurons and to explore the functional role of I_{Af} in shaping action potential waveforms and controlling repetitive firing patterns. Using the biolistic gene gun, cDNAs encoding a dominant negative mutant Kv4.2 α-subunit (Kv4.2W362F) and enhanced green fluorescent protein (EGFP) were introduced into rat sympathetic neurons *in vitro*. Whole-cell voltage-clamp recordings obtained from EGFP-positive cells revealed that I_{Af} is selectively eliminated in cells expressing Kv4.2W362F, demonstrating that Kv4 α-subunits underlie I_{Af} in sympathetic neurons.

In addition, I_{Af} density is increased significantly in cells overexpressing wild-type Kv4.2. In cells expressing Kv4.2W362F, input resistances are increased and (current) thresholds for action potential generation are decreased, demonstrating that I_{Af} plays a pivotal role in regulating excitability. Expression of Kv4.2W362F and elimination of I_{Af} also alters the distribution of repetitive firing patterns observed in response to a prolonged injection of depolarizing current. The wild-type superior cervical ganglion is composed of phasic, adapting, and tonic firing neurons. Elimination of I_{Af} increases the percentage of adapting cells by shifting phasic cells to the adapting firing pattern, and increased I_{Af} density reduces the number of adapting cells.

Key words: K^+ channels; I_A; Kv4 α-subunits; Kv4.2W362F; transgenics; gene gun; neuronal excitability; repetitive firing patterns

Voltage-gated potassium (K^+) currents are key regulators of excitability in mammalian neurons, and in most cell types, two broad classes of voltage-gated K^+ currents have been distinguished: (1) rapidly activating and inactivating currents, I_A, and (2) delayed rectifier K^+ currents, I_K (Rudy, 1988; Storm, 1990). These are broad classifications, however, and in most mammalian neurons, multiple K^+ current components with distinct time- and voltage-dependent properties have been identified. This diversity has physiological significance because the various K^+ currents contribute to determining the waveforms of individual action potentials and repetitive firing patterns (Pongs, 1999). Molecular cloning of K^+ channel pore-forming α- and β-subunits has revealed considerably more heterogeneity (Coetzee et al., 1999) than was expected based on the physiology, and the relationships between these subunits and functional neuronal voltage-gated K^+ channels are not well understood.

At present, there is considerable interest in determining the molecular correlates of functional voltage-gated K^+ channels in mammalian neurons and in defining the roles of these channels in shaping action potential waveforms, repetitive firing patterns, and responses to synaptic inputs (Coetzee et al., 1999). In the experiments here, a molecular genetic approach has been exploited to address these issues in neurons isolated from the superior cervical ganglion (SCG) of the rat. Previous studies have documented the expression of (at least) three voltage-gated outward K^+ currents in rat SCG neurons: a fast transient 4-aminopyridine (4-AP)-sensitive current (I_A), a slowly activating and inactivating tetraethylammo-

nium (TEA)-sensitive delayed rectifier current (I_K), and, a steady-state component (Freshi, 1983; Galvan and Sedlmeir, 1984; Belluzzi et al., 1985a,b). A number of voltage-gated K^+ channel (Kv) pore-forming α-subunits, including Kv1.1, 1.2, 1.3, 1.4, 2.1, 2.2, 4.1, 4.2, and 4.3, that likely contribute to these currents have been shown to be expressed in rat SCG (Dixon and McKinnon, 1996; Pankevych et al., 1999). Of these subunits, only Kv1.4 and Kv4.1, Kv4.2, and Kv4.3 produce rapidly activating and inactivating 4-AP-sensitive currents (Coetzee et al., 1999) that resemble the transient outward current I_A in SCG neurons.

Previous studies have demonstrated that α-subunits of the Kv4 subfamily underlie the fast component of the transient current $I_{to,f}$ in cardiac cells (Fiset et al., 1997; Johns et al., 1997; Barry et al., 1998; Xu et al., 1999a), and several lines of evidence suggest that Kv4 α-subunits play a role in the generation of I_A in central neurons (Serodio et al., 1994; Baro et al., 1997; Johns et al., 1997; Martina et al., 1998; Song et al., 1998; Tkatch et al., 2000). The experiments here were undertaken, therefore, to test directly the hypothesis that Kv4 α-subunits contribute to I_A in sympathetic neurons by examining the effects of expression of a mutant Kv4 α-subunit, Kv4.2W362F, that functions as a dominant negative (Barry et al., 1998). The results reveal that the fast transient current, I_{Af}, is eliminated in SCG cells expressing Kv4.2W362F. Experiments focused on exploring the functional consequences of elimination of I_{Af} on the waveforms of action potentials and the repetitive firing properties of SCG cells are also presented.

MATERIALS AND METHODS

Culture of SCG neurons. Sympathetic neurons were isolated from the SCG of embryonic day 21 (E21) to postnatal day 1 (P1) Long–Evans rat pups using a procedure similar to that described by Chang et al. (1990). Briefly, after anesthesia with 5% halothane, animals were decapitated, and the SCG was removed. Ganglia were successively incubated for 30 min periods in collagenase and trypsin at room temperature; isolated SCG neurons were obtained by trituration and subsequent centrifugation. Dissociated SCG cells were resuspended in growth medium [Earle's Minimum Essential Medium (EMEM) with 10% fetal calf serum (FCS), 0.14 mM L-glutamine, 100 U/ml penicillin/streptomycin and 0.05 mM NGF] and plated at a density of $2.5 \times 10^4/cm^2$ on glial monolayers [prepared as in Raff et al. (1979)]. Cells were maintained in a 95% O_2/5% CO_2 37°C

incubator, and the medium was exchanged with fresh growth medium approximately every 48 hr.

Immunohistochemistry. The affinity-purified rabbit polyclonal anti-Kv4 pan antibody used in this study was raised against residues 484–502 in the C terminus of Kv4.2, and it has been shown to reliably detect Kv4.2 and Kv4.3 (Barry et al., 1995). The corresponding sequence in Kv4.1 is similar (~80% identical to the Kv4.2 sequence), and it is assumed that this antibody will also recognize Kv4.1. Polyclonal antibodies generated against unique sequences in Kv4.2 and Kv4.3 were also used. The Kv4.3-specific antibody was targeted against residues 450–467 in the C-terminal region of Kv4.3 and has been shown previously to detect Kv4.3 with no detectable cross-reactivity with Kv4.2 (Brahmajothi et al., 1999). The anti-Kv4.2 antibody was generated against amino acid residues 29–38 in the N terminus of Kv4.2. As in previous studies (Barry et al., 1995; Brahmajothi et al., 1999; Pond et al., 2000), antibody specificity and cross-reactivity were assessed by immunohistochemical and Western blot analysis of cells transiently expressing Kv4.2, Kv4.3, or another Kv α-subunit. The anti-Kv4.2 antibody only detects Kv4.2; no cross-reactivity is observed (R. Hood, B. K. Scheve, and J. M. Nerbonne, unpublished observations). A mouse monoclonal anti-FLAG M2 antibody (Kodak) was used (at a 1:500 dilution) to detect the Kv4.2W362F-FLAG protein in transfected SCG neurons. For immunohistochemistry, cells were fixed in 4% paraformaldehyde for 30 min, incubated in blocking buffer (PBS containing 5% normal goat serum, 0.02% Triton X-100, and 0.1% NaNH$_3$) for 1 hr and labeled with a primary antibody (1:100 dilution) at 4° overnight. After washing, cultures were incubated with a Cy3-labeled goat anti-rabbit (or rabbit anti-mouse) IgG secondary antibody (Chemicon, Temecula, CA). After washing, labeled cells were visualized with laser illumination using a Zeiss inverted confocal microscope, and images were captured in 1 μm sections.

Transfection of isolated SCG neurons with the gene gun. In preliminary experiments, 1.6 μm gold beads were coated with pCMV-EGFP (Clonetech), which encodes enhanced green fluorescent protein (EGFP), and propelled (450 psi; 2 mm carrier distance) into SCG neurons at 4 d *in vitro* using the gene gun (Bio-Rad), a biolistic projectile system. After transfections, the cultures appeared healthy, and expression of EGFP was readily detected 24 hr later (see Results). In experiments aimed at examining the effects of Kv4.2W362F or Kv4.2 expression in SCG neurons, the gold particles were coated with either pBK-CMV-Kv4.2 and pCMV-EGFP or pBK-CMV-Kv4.2W362F-FLAG and pCMV-EGFP in a 4:1 ratio (total of 10 μg of DNA). Because EGFP expression was used to identify transfected neurons for subsequent electrophysiological characterization, immunohistochemical experiments were performed to determine whether EGFP-expressing cells also expressed the Kv4.2W362F-FLAG construct (see Results).

Electrophysiological recording. Whole-cell recordings were obtained from isolated SCG neurons at room temperature (22–25°C). Data were collected using an Axopatch-1B patch-clamp amplifier; experimental parameters were controlled with a P5–120 Gateway2000 computer through a TL-1 DMA Interface using the PClamp7 software package (Axon Instruments). Electrodes were fabricated from soda-lime glass (Chase 2502) with a two-stage puller, and the shanks were coated with a silicone elastomer (Sylgard, Dow Corning, Corning, NY). Pipette resistances were 1.5–3 MΩ after fire-polishing. For voltage-clamp recordings, the bath solution routinely contained (in mM): 140 NaCl, 4 KCl, 2 CaCl$_2$, 2 MgCl$_2$, 10 HEPES, 5 glucose, 0.001 TTX, and 0.1 CdCl$_2$ (pH 7.5, 300 mOsm). Recordings were also obtained from SCG neurons in the current-clamp mode, and the TTX and CdCl$_2$ were omitted from the bath for these studies. The pipette solution for both current and voltage-clamp recordings contained (in mM): 135 KCl, 10 HEPES, 5 glucose, 3 MgATP, 0.5 NaATP, 2 EGTA, 1.1 CaCl$_2$ (pH 7.5, 300 mOsm). Series resistances, estimated from the decays of the uncompensated capacitative transients, were 2–5 MΩ and were compensated electronically by ~80–90%. Because current amplitudes were <10 nA, the voltage errors resulting from the uncompensated series resistance were always <10 mV and were not corrected. Voltage-gated K$^+$ currents were evoked during 125 msec or 6 sec depolarizing voltage steps to test potentials between −40 mV and +50 mV from a holding potential of −90 mV. Single action potentials and action potential trains were recorded in response to brief (1.5 msec) 200–400 pA and prolonged (500 msec) 20–200 pA depolarizing current injections.

Data analysis. Data were compiled and analyzed using pCLAMP7 (Axon) and Excel (Microsoft) software and are presented as means ± SEM. To ensure adequate spatial control of the membrane voltage, the decay phase of the capacitative transients were analyzed, and only cells in which >90% of the amplitude of the capacitative transient decayed with a single exponential time course were included in this study. Only data obtained from cells with an input resistance >100 MΩ were analyzed and included here. The mean (±SEM) input resistance and capacitance of EGFP-expressing SCG neurons were 0.34 ± 0.03 GΩ and 32 ± 2 pF (*n* = 43), respectively. Leak currents were <100 pA (at −70 mV) and were not subtracted. To determine the amplitudes and the decay time constants of the individual components of the total depolarization-activated outward K$^+$ currents in SCG neurons, the inactivation phases of the currents recorded during prolonged (6 sec) depolarizations were analyzed using the equation $y = A_1 e^{-t/\tau 1} + A_2 e^{-t/\tau 2} + A_3 e^{-t/\tau 3} + C$, where A_1, A_2, and A_3 (measured in pA/pF) are the amplitudes of the inactivating current components (I_{Af}, I_{As}, and I_K) that decay with τ_1, τ_2, and τ_3 (measured in milliseconds), respectively, and C is the steady-state current (measured in
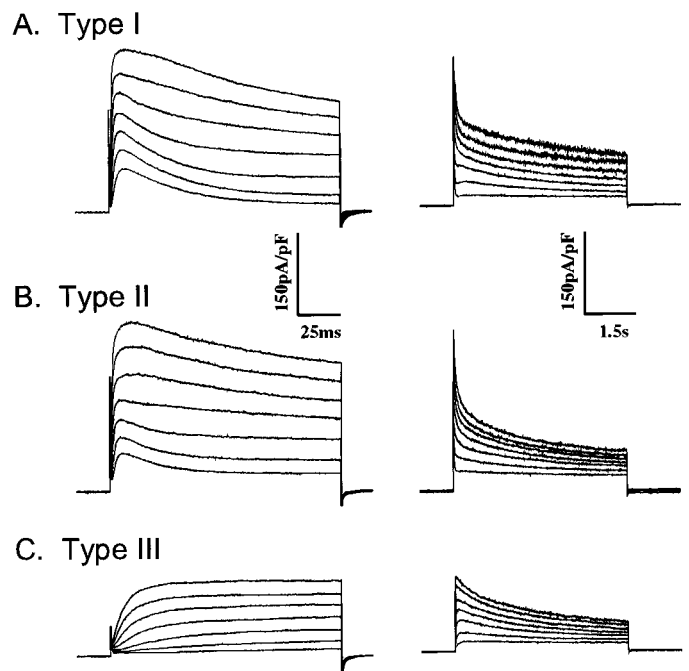

A. Type I

B. Type II

C. Type III

Figure 1. Voltage-gated outward K$^+$ current waveforms in SCG neurons. Whole-cell outward K$^+$ currents were recorded from isolated SCG neurons in response to 125 msec (*left panels*) and 6 sec (*right panels*) depolarizing voltage steps from a holding potential of −90 mV. Experiments were conducted as described in Materials and Methods with 1 μM TTX and 100 μM CdCl$_2$ in the bath solution to block voltage-gated inward Na$^+$ and Ca^{2+} currents, respectively. The *left* and *right* panels in *A–C* were recorded from the same cell. There are distinct and stereotyped differences in the waveforms of the currents in Type I, II, and III cells (see Results and Table 1). There is a prominent rapid component of current decay in Type I (*A*) and II (*B*) cells that is not evident in Type III (*C*) cells; current activation is also slower in Type III (*C*) cells (see Results).

pA/pF) remaining at the end of the 6 sec depolarization (see Results). Fits were obtained using CLAMPFIT6, and best fits were determined by eye (in all cases, σ < 30 pA). All current-clamp recordings were obtained from cells with overshooting action potentials and stable resting membrane potentials negative to −50 mV. Action potential durations were measured at 50% (APD$_{50}$) and 90% (APD$_{90}$) repolarization. Statistical significance was examined with the Student's *t* test, and where appropriate, *p* values are presented in the text.

RESULTS

Multiple components of the outward K$^+$ currents in SCG neurons

In the experiments here, neurons were isolated from the SCG of E21 or P1 rats, plated on glial monolayers, and maintained *in vitro*. Whole-cell voltage-gated K$^+$ currents were recorded in the presence of 1 μM TTX and 0.1 mM CdCl$_2$ to block voltage-gated Na$^+$ and Ca^{2+} currents, respectively. Representative outward currents recorded from (three) isolated SCG neurons in response to brief (125 msec) and prolonged (6 sec) membrane depolarizations to varying test potentials from a holding potential of −90 mV are presented in Figure 1. The rates of rise and the amplitudes of the currents increase with increasing membrane depolarization; the largest and most rapidly activating current in each panel of Figure 1 was evoked at +50 mV. No voltage-gated K$^+$ currents were recorded when the K$^+$ in the recording pipettes was replaced with Cs$^+$ (*n* = 9). The currents recorded (Fig. 1) and analyzed here, therefore, are assumed to reflect only the currents through Ca^{2+}-independent voltage-gated K$^+$ channels.

As is clearly evident in Figure 1, the amplitudes and the waveforms of the outward K$^+$ currents vary markedly among SCG neurons. Nevertheless, outward K$^+$ current waveforms in SCG cells are stereotyped, and the records shown in Figure 1*A–C* are representative of the three distinct phenotypes observed; these are referred to as Type I (*A*), II (*B*), or III (*C*). In the majority

Table 1. Outward K⁺ currents in wild-type and transfected SCG neurons[a]

Phenotype		Wild type			Kv4.2W362F			Kv4.2	
		Type I	Type II	Type III	A	B	C	Type I	Type II
Peak current density		252 ± 20	259 ± 22	211 ± 18	162 ± 21	289 ± 31	244 ± 35	249 ± 27	291 ± 37
I_{Af}	density (pA/pF)	81 ± 11	111 ± 21				64 ± 20	127 ± 9[+]	136 ± 16[+]
	τ (msec)	121 ± 14	95 ± 8				190 ± 18	87 ± 10	70 ± 8
I_{As}	density (pA/pF)		45 ± 3			67 ± 15			57 ± 21
	τ (msec)		480 ± 21			490 ± 31			472 ± 8
I_{K}	density (pA/pF)	108 ± 12	64 ± 9*	136 ± 11	111 ± 22	157 ± 25**	115 ± 7	78 ± 17[++]	67 ± 2
	τ (msec)	2560 ± 187	2800 ± 193	2200 ± 176	2050 ± 235	2473 ± 254	2368 ± 197	2126 ± 518	2151 ± 195
I_{SS}	density (pA/pF)	74 ± 5	45 ± 5*	79 ± 6	65 ± 9	72 ± 15	68 ± 15	40 ± 6[++]	38 ± 17
n		30	9	4	18	7	6	11	5

*I_K and I_{SS} densities are significantly ($p < 0.005$) lower in wild-type Type II than in either wild-type Type I or III cells. **I_K density is significantly ($p < 0.002$) higher in Kv4.2W362F-expressing cells than in wild-type Type II cells. [+]I_{Af} density is significantly ($p < 0.04$) greater in Kv4.2-expressing cells than in wild-type Type I or II cells. [++]I_K and I_{SS} densities are also significantly ($p < 0.005$) lower in Kv4.2-expressing cells than in wild-type Type I cells (Table 1).
[a]All values are mean ± SEM; current densities determined at +50 mV; n = number of cells.

(>90%) of cells studied, currents similar to those in Figure 1, *A* and *B*, were recorded. There is a prominent rapid component of current decay in these (Type I and Type II) cells (*right panels*), consistent with the presence of a fast transient outward "A" K⁺ current (Belluzzi et al., 1985a; Storm, 1990; McFarlane and Cooper, 1992). This current is referred to here as $I_{A,fast}$, or I_{Af}, to distinguish it from another, more slowly inactivating, transient outward K⁺ current $I_{A,slow}$ (I_{As}) that is also seen in some SCG cells (see below). Analysis of the outward K⁺ currents evoked during long depolarizations in Type I SCG cells (Fig. 1*A, right panel*) revealed that current decay is well described by the sum of two exponentials, with decay time constants (τ_{decay}) that differ by more than an order of magnitude, and a noninactivating steady-state current (see below). The mean ± SEM τ_{decay} ($n = 30$) determined for the fast and slow components of decay in these (Type I) cells were 121 ± 14 and 2560 ± 187 msec, respectively (Table 1). Neither time constant displays any appreciable voltage dependence (data not shown). Two K⁺ currents with similar τ_{decay} values have been described previously in rat sympathetic neurons and were assumed to reflect the expression of distinct K⁺ channels (McFarlane and Cooper, 1992). The rapidly inactivating current has been referred to as I_A, or I_{Af} (Freshi, 1983; Galvan and Sedlmeir, 1984; Belluzzi et al., 1985a; Nerbonne et al., 1986; McFarlane and Cooper, 1992; Wang and McKinnon, 1995), and the slowly inactivating current has been given various names, including I_K (Galvan and Sedlmeir, 1984; Belluzzi et al., 1985b; Nerbonne and Gurney, 1989) and $I_{A,slow}$ (McFarlane and Cooper, 1992). The very slowly decaying current component ($\tau_{decay} = 2560 \pm 187$ msec) is referred to here as I_K to emphasize the slow inactivation kinetics and to distinguish this conductance pathway from I_{As} (see below).

Although the waveforms of the currents in individual (Type I) SCG cells are similar, the densities of I_{Af} and I_K vary considerably. For example, I_{Af} density at +50 mV ranged from 70 to 208 pA/pF, with a mean ± SEM of 81 ± 11 pA/pF ($n = 30$) (Table 1). Similarly, I_K densities at +50 mV in Type I cells varied considerably, ranging from 83 to 258 pA/pF with a mean ± SEM of 108 ± 12 pA/pF (Table 1). The density of the noninactivating K⁺ current component remaining at the end of 6 sec voltage steps (Fig. 1), I_{SS} (steady-state), is also variable; at +50 mV, for example, I_{SS} density ranged from 35 to 127 pA/pF, with a mean ± SEM of 74 ± 5 pA/pF ($n = 30$) (Table 1).

In some (9) of the 43 SCG cells studied, outward K⁺ current waveforms similar to those displayed in Figure 1*B* were observed. In these (Type II) cells, the decay phases of the outward K⁺ currents were not well described by biexponential functions, and three exponentials were required to adequately describe the data. The mean ± SEM τ_{decay} values derived from these fits were 95 ± 8, 480 ± 21, and 2800 ± 193 msec (Table 1). The fast τ_{decay} (95 ± 8 msec) and the very slow τ_{decay} (2800 ± 193 msec) are not

significantly different from those determined for I_{Af} and I_K, respectively, in Type I cells. It is assumed, therefore, that these time constants also reflect expression of I_{Af} and I_K in Type II cells (see below). The component of current inactivation in Type II cells with a $\tau_{decay} = 480 \pm 21$ msec is referred to as $I_{A,slow}$, or I_{As}, and is assumed to reflect the expression of a novel conductance pathway, distinct from $I_{A,fast}$, I_K, and I_{SS} (see below and Discussion). Although I_{Af} densities are similar in Type I and Type II cells, the densities of I_K and I_{SS} are significantly ($p < 0.005$) lower in Type II than in Type I cells (Table 1).

In the other four (of 43 or ~9%) SCG cells (Type III) studied, no rapidly inactivating K⁺ currents (similar to I_{Af} and/or I_{As}) were evident (Fig. 1*C*). The decay phases of the outward currents in these cells were well described by a single exponential with a mean ± SEM τ_{decay} of 2200 ± 176 msec (Table 1). Peak outward K⁺ current densities in Type III cells, which lack both I_{Af} and I_{As} (Table 1), are lower than in Type I and II cells (Table 1). In addition, in Type III cells, I_{SS} contributes substantially more to the peak outward current than does I_{SS} in Type I or II cells (Table 1). In other respects, however, the properties of Type III cells are indistinguishable from Type I and II cells. The mean ± SEM whole-cell membrane capacitances and input resistances, for example, were 33 ± 3 pF and 0.52 ± 0.08 GΩ for the cells with I_{Af} ($n = 39$), and 25 ± 2 pF and 0.60 ± 0.04 GΩ for the cells lacking I_{Af} ($n = 4$).

I_{Af} is selectively attenuated in SCG neurons expressing Kv4.2W362F

On the basis of the kinetic properties of I_{Af} and the sensitivity of this current to 4-AP, it seemed reasonable to suggest that this conductance pathway reflects the expression of Kv4 α-subunits. Consistent with this hypothesis, previous studies have documented the expression of Kv4.1, Kv4.2, and Kv4.3 mRNAs in SCG neurons (Dixon and McKinnon, 1996; Pankevych et al., 1999). In addition, immunohistochemical experiments with anti-Kv4 α-subunit-specific antibodies reveal the expression of these subunits in isolated SCG neurons (Fig. 2). As evident in Figure 2*A*, for example, Kv4.2 expression is readily detected in the cell bodies of isolated SCG neurons. The expression pattern for Kv4.3 is distinct (from that of Kv4.2): Kv4.3 staining is seen throughout the processes of isolated SCG neurons (Fig. 2*B*). In addition, the anti-Kv4.3 labeling appears to be punctate (Fig. 2*B*), suggesting "clustering" of Kv4.3-encoding K⁺ channels. A similar staining pattern is seen with an anti-Kv4 pan antibody, which also strongly labels cell bodies and proximal processes (Fig. 2*C*).

To test the hypothesis that Kv4 α-subunits underlie I_{Af} in SCG neurons, cells were transfected with a pore mutant of Kv4.2, Kv4.2W362F, that functions as a dominant negative (Barry et al., 1998). Previous studies have shown that coexpression of
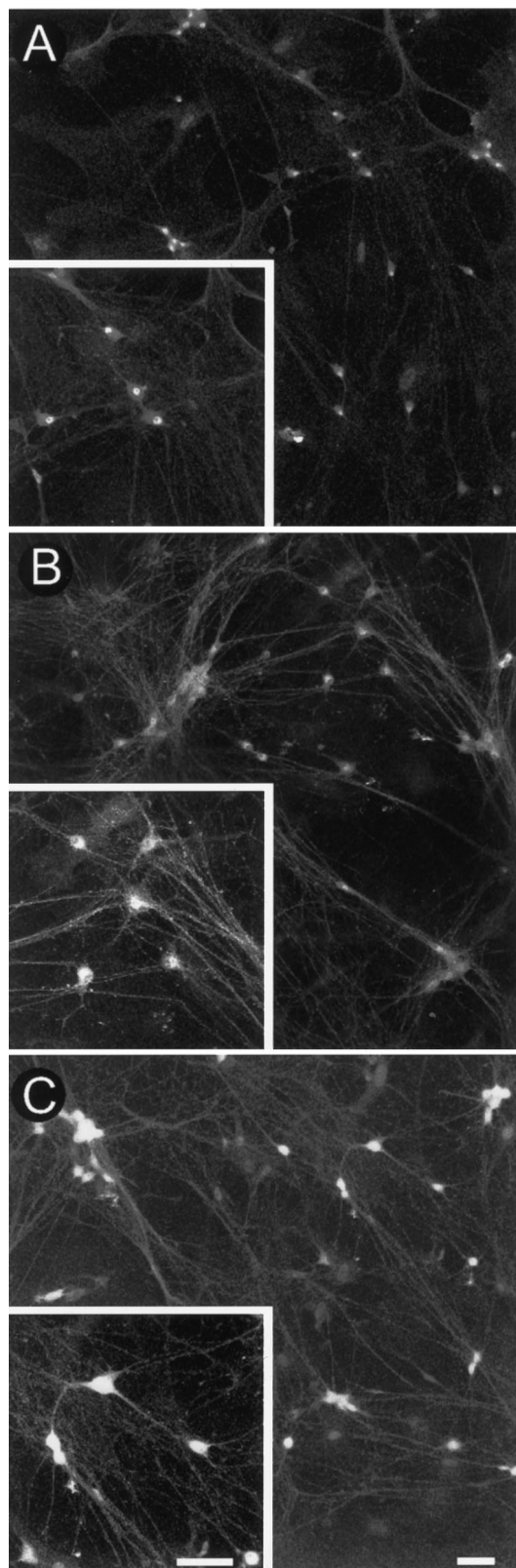
Figure 2. Expression of Kv4 α-subunits in SCG neurons. Isolated wild-type SCG neurons were examined immunohistochemically 48 hr after plating, as described in Materials and Methods. Cultures were stained with anti-Kv4.2 (*A*), anti-Kv4.3 (*B*), and a pan-Kv4 antibody (*C*). Both Kv4.2 and Kv4.3 are readily detected in SCG neurons; Kv4.2 is localized to the cell bodies and proximal processes, whereas Kv4.3 is also detected in more distal processes. In addition, the anti-Kv4.3 appears more punctate. Scale bars, 50 μm.
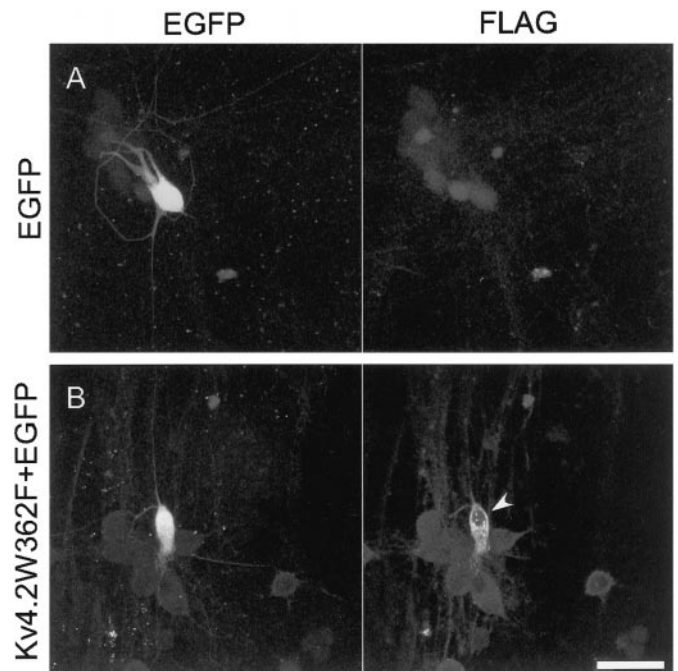

Figure 3. Immunohistochemical detection of Kv4.2W362F-FLAG in transfected SCG neurons. Isolated SCG neurons, transfected with EGFP alone (*A*) or with Kv4.2W362F-FLAG and EGFP (*B*) using the gene gun, were fixed and stained 24 hr later (see Materials and Methods). *A, B*, EGFP fluorescence (*left panels*) and Cy3 fluorescence (*right panels*) images of the same field. Anti-FLAG staining is only evident in cultures transfected with Kv4.2W362F-FLAG expression (compare *right panels* in *A* and *B*). In addition, EGFP expression correlates with Kv4.2W362F (compare *left* and *right panels* in *B*). Scale bar, 50 μm.

Kv4.2W362F with either Kv4.2 or Kv4.3 attenuates current amplitudes relative to cells expressing (wild-type) Kv4.2 or Kv4.3 alone (Barry et al., 1998). In the experiments here, beads were coated either with cDNA constructs encoding Kv4.2W362F and EGFP or with the EGFP cDNA alone, and cells were transfected using the biolistics gene gun (see Materials and Methods). Within ~24 hr of transfection, EGFP expression was readily detected under epifluorescence illumination (Fig. 3*A*); ~10% of the cells in these cultures were EGFP positive. To determine whether EGFP-positive cells in cultures exposed to beads coated with Kv4.2W362F (and EGFP) also express the transgene, the cultures were fixed ~48 hr after transfection and probed with the anti-FLAG M2 antibody. These experiments revealed that all EGFP-positive cells in these cultures (*n* = 112) also express Kv4.2W362F-FLAG. An example of an EGFP-positive, Kv4.2W362F-positive cell is illustrated in Figure 3*B*. As is evident, the FLAG staining appears to be predominantly on the cell surface (*arrow*), whereas EGFP expression is detected in the cytosol (Fig. 3*B*). In addition, EGFP appears to fill the entire cell (Fig. 3*B*).

Representative whole-cell voltage-gated outward K$^+$ current waveforms recorded from SCG neurons expressing Kv4.2W362F (and EGFP) are presented in Figure 4. Control experiments revealed that the outward K$^+$ currents in cells expressing EGFP alone are indistinguishable from those in wild-type cells (Fig. 1). The waveforms of the outward K$^+$ currents in cells expressing Kv4.2W362F (Fig. 4), however, are very different from those recorded from wild-type cells. Specifically, the rapid component of current decay, I_{Af}, that is prominent in wild-type Type I (Fig. 1*A*) and Type II (Fig. 1*B*) SCG cells appears to be missing in (all) cells expressing Kv4.2W362F (Fig. 4). In contrast to the results obtained on wild-type and EGFP-expressing cells (Table 1), the decay phases of the outward currents in the majority (18 of 31, 58%) of Kv4.2W362F-expressing cells (Fig. 4*A*) were well described by a single exponential (τ_{decay} = 2205 ± 235 msec) and a steady-state outward current (Table 1). The waveforms of the currents in these
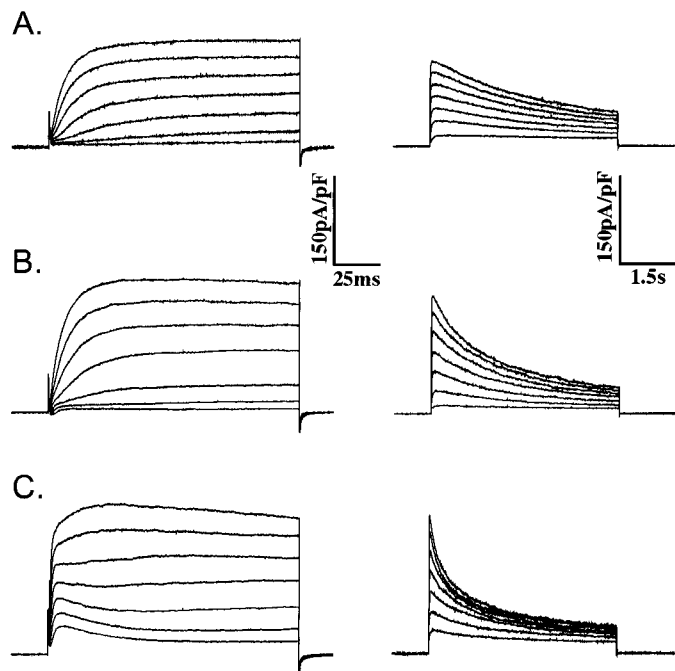
A.

B.

C.

Figure 5. Two components of I_{Af} in SCG neurons. The time constants of inactivation of the rapid component of current decay were determined in wild-type, Kv4.2W362F-, and Kv4.2-expressing SCG cells, as described in Materials and Methods. The τ_{decay} values were binned in 40 msec increments for comparison purposes, and, as is evident, the distributions of τ_{decay} values are distinct (see Results).

Figure 4. I_{Af} is eliminated in SCG neurons expressing Kv4.2W362F-FLAG. Whole-cell depolarization-activated outward K$^+$ currents were recorded from isolated SCG neurons transfected with Kv4.2W362F-FLAG as described in the legend to Figure 1. The *left* and *right panels* in *A–C* were recorded from the same cell. The waveforms of the currents recorded from cells expressing Kv4.2W362F are distinct from those recorded from wild-type cells or from cells expressing EGFP alone (Fig. 1). In the majority of cells (*A, B*), current activation and inactivation are slow, consistent with the absence of I_{Af} (see Results). In a small subset of Kv4.2W362F-expressing cells (*C*), a rapid component of decay with a mean ± SEM τ_{decay} that is not significantly different from that determined for I_{Af} in wild-type Type I SCG cells (Table 1) is evident (see Results).

Figure 6. Distinct repetitive firing patterns in SCG neurons. Action potentials and repetitive firing patterns were recorded from isolated EGFP-expressing SCG neurons in response to brief or prolonged depolarizing current injections, as described in Materials and Methods. Current-clamp recordings from three representative cells are shown in *A–C*. In each cell, single action potentials were elicited by 1.5 msec depolarizing current injections (*left panels*), and repetitive firing patterns were recorded in response to 500 msec depolarizing currents injections of 100 pA (*middle panels*) or 200 pA (*right panels*). Based on the response(s) to the 500 msec current injections, cells were classified as phasic (*A*), adapting (*B*), or tonic (*C*) (see Results and Table 2).

cells (Fig. 4*A*) are indistinguishable from wild-type Type III cells (Fig. 1*C*), suggesting expression of only I_K and I_{SS} (Table 1). In the remaining Kv4.2W362F-expressing cells (Fig. 4*B,C*), two exponentials were required to fit the decay phases of the currents. In 7 of 31 cells, current waveforms similar to those in Figure 4*B* were recorded. Analysis of the decay phases of the outward K$^+$ currents in these cells provided mean ± SEM τ_{decay} values of 490 ± 31 and 2473 ± 254 msec, consistent with the presence of I_{As} and I_K; I_{SS} is also evident in these cells (Table 1). Although these (Fig. 4*B*) cells represent a novel (nonphysiological) class of SCG neurons, the percentage (22%) of cells with this phenotype and the distribution of current densities suggest that these are Type II cells that lack the fast transient current component, I_{Af}, attributable to the expression of Kv4.2W362F. Interestingly, the densities of I_K and I_{SS} in these cells (Table 1) are significantly ($p < .002$) higher than in wild-type Type II cells (Table 1), suggesting that I_K and I_{SS} are upregulated in Type II cells when I_{Af} is eliminated (see Discussion).

In the remaining Kv4.2W362F-expressing SCG cells ($n = 6$), a rapid component of outward current decay is detected (Fig. 4*C*), suggesting that I_{Af} is unaffected by Kv4.2W362F expression in a subset of SCG cells. Analysis of the currents in records such as those in Figure 4*C* revealed that the mean ± SEM density of this component is lower and the mean ± SEM τ_{decay} is longer than those determined for I_{Af} in wild-type Type I and II cells (Table 1). These observations suggest that there are actually two components of I_{Af}, only one of which is encoded by Kv4 α-subunits (and therefore affected by Kv4.2W362F expression) or, alternatively, that a novel current is upregulated in this subset of SCG cells (Fig. 4*C*) when I_{Af} is eliminated. The time constants of inactivation of currents in records such as those in Figure 4*C* varied over the range 138–249 msec. Although this range is similar to that (60–208 msec) observed in wild-type Type I and II cells, it is narrower, and the distributions of time constants are quite different (Fig. 5). In the
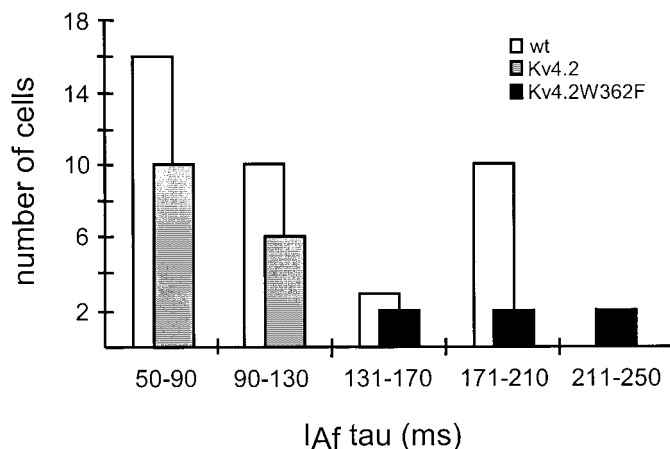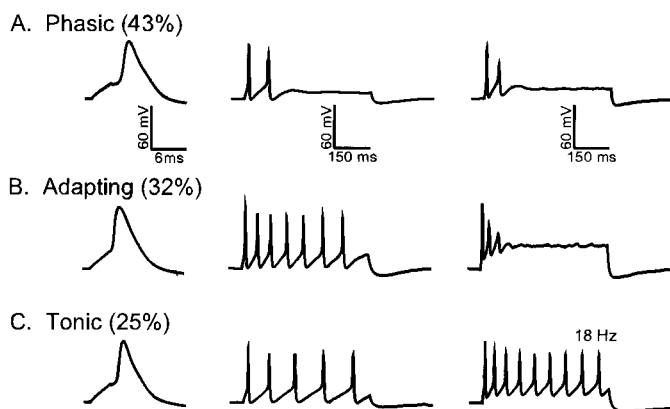
Kv4.2W362F-expressing cells, τ_{decay} values fall between 138 and 249 msec, whereas in wild-type cells, there appear to be two distinct groups of cells, i.e., those with τ_{decay} values in the 50–130 msec range (26 of 39; 66%) and those with τ_{decay} values between 131 and 210 msec (13 of 39; 33%). These observations further suggest that only the faster current (τ_{decay} 50–130 msec) is encoded by Kv4 α-subunits (see Discussion).

Action potential waveforms and repetitive firing in SCG neurons

Subsequent experiments were aimed at evaluating the role of I_{Af} in shaping the waveforms of individual action potentials and in determining the repetitive firing properties of SCG neurons. Although the waveforms of the action potentials recorded from wild-type SCG neurons are similar, the responses to prolonged (500 msec) depolarizing current injections are distinct (Fig. 6*A–C*). In ~45% of the SCG cells examined, phasic firing was observed, i.e., cells fire one or two action potentials in response to prolonged current injections (Fig. 6*A*, *middle panel*), and the number of action potentials elicited is unaffected by increasing the amplitude of the

Table 2. Resting and active membrane properties of SCG neurons[a]

Phenotype	R_{in} (GΩ)	V_m (mV)	AP$_{Thresh}$ (pA)	APA (mV)	APD$_{50}$ (msec)	APD$_{90}$ (msec)	n
All cells	0.34 ± 0.03	−48 ± 1	46 ± 5	82 ± 4	3.66 ± 0.14	5.92 ± 0.20	28
Phasic	0.26 ± 0.02	−45 ± 2	67 ± 1	80 ± 5	4.18 ± 0.24	6.55 ± 0.34	12
Adapting	0.60 ± 0.06**	−48 ± 1	24 ± 2*	87 ± 3	3.57 ± 0.20	5.96 ± 0.20	9
Tonic	0.22 ± 0.02	−52 ± 1	42 ± 2	91 ± 3	2.97 ± 0.03++	4.87 ± 0.20+	7

*,**Values are significantly different from those in phasic or tonic cells at the $p < 0.003$* and $p < 0.001$** levels; +,++values are significantly different from those in phasic cells ($p < 0.001$++) and from those in phasic or adapting cells ($p < 0.003$+).

[a]All values are means ± SEM.

injected current (Fig. 6*A*, *right panel*). Repetitive firing was observed, however, in the remaining ~55% of the SCG cells studied (Fig. 6*B,C*). In approximately half of these cells, low amplitude current injections produce repetitive firing, and the frequency of firing decreases as a function of time after the onset of the current injection, i.e., these cells "adapt" (Fig. 6*B*, *middle panel*). When the amplitude of the injected current is increased, adapting cells become refractory and firing ceases, despite the maintained current injection (Fig. 6*B*, *right panel*). The remaining subset of cells displayed "tonic" activity, firing regularly spaced action potentials in response to prolonged depolarizing current injections (Fig. 6*C*, *middle panel*). In addition, in tonic cells, the frequency of firing increases with the amplitude of the injected current (Fig. 6*C*, *right panel*). No refractoriness is evident in tonic cells during current injections ranging from 20 to 300 pA, clearly distinguishing these cells from both phasic and adapting neurons.

The properties of phasic, adapting, and tonic cells are quite similar, despite the marked differences in repetitive firing patterns (Fig. 6). Resting membrane potentials and action potential amplitudes, for example, are indistinguishable in phasic, adapting, and tonic SCG cells (Table 2). Action potentials recorded from tonic cells, however, are significantly ($p < 0.001$) briefer than in either phasic or adapting cells (Table 2). At 90% repolarization, for example, the mean ± SEM action potential duration (APD$_{90}$) in tonic cells is 4.87 ± 0.20 msec, whereas mean ± SEM APD$_{90}$ values determined in phasic and tonic cells were 5.96 ± 0.20 and 6.55 ± 0.34 msec, respectively (Table 2). In addition, the input resistances of adapting cells are significantly ($p < 0.001$) higher than those of either phasic or tonic cells (Table 2). Consistent with this difference in input resistance, the mean ± SEM current threshold (24 ± 2 pA) for action potential generation is significantly ($p < 0.003$) lower in adapting cells than in phasic (67 ± 1 pA) or tonic (42 + 2 pA) cells (Table 2). Subsequent experiments were aimed at determining directly the role of I_{Af} in mediating the phasic, tonic, and adapting firing patterns of SCG neurons by examining the effects of Kv4.2W362F expression on action potentials and repetitive firing.

Elimination of I_{Af} increases excitability (and percentage) of "adapting" SCG cells

Previous pharmacological studies suggest a primary role for I_{Af} in the regulation of excitability and in action potential repolarization in SCG neurons (Galvan and Sedlmeir, 1984; Belluzzi et al., 1985a; Nerbonne and Gurney, 1989). Application of 4-AP, often assumed to be a specific blocker of I_{Af}, for example, reportedly increases the excitability of SCG neurons (Galvan and Sedlmeir, 1984). In the presence of 4-AP, the current threshold for action potential generation and the latency to firing are reduced, and action potentials are prolonged (Galvan and Sedlmeir, 1984; Belluzzi et al., 1985a; Nerbonne and Gurney, 1989). In some studies, the input resistances of SCG neurons were also reportedly increased after exposure to 4-AP (Galvan and Sedlmeir, 1984; Belluzzi et al., 1985a). If all of these effects are attributable to loss of I_{Af}, then similar changes in excitability and action potential durations would be expected to be observed in SCG neurons expressing Kv4.2W362F (and lacking I_{Af}).

Representative current-clamp recordings from SCG cells expressing Kv4.2W362F are presented in Figure 7. As in recordings
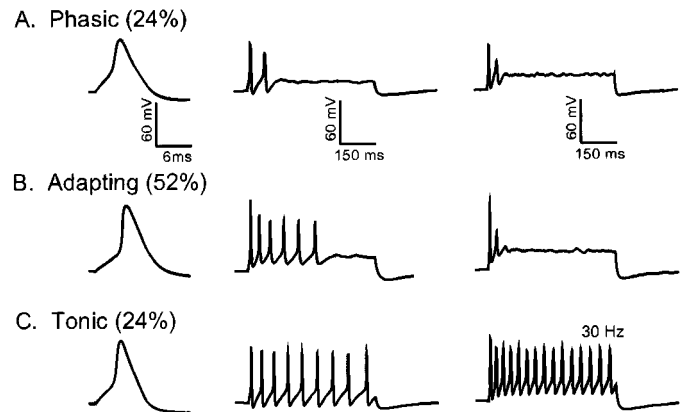

Figure 7. Elimination of I_{Af} increases the percentage of adapting cells. Action potentials and repetitive firing patterns were recorded, as described in the legend to Figure 6, from isolated SCG neurons expressing Kv4.2W362F. Records from three representative cells are shown in *A–C*. As in wild-type cells (Fig. 6), the phasic, adapting, and tonic firing patterns are observed in Kv4.2W362F-expressing cells. However, the percentage of adapting cells is increased markedly, and the percentage of phasic cells is decreased (Table 3) relative to the distribution of firing patterns in wild-type cells (Table 2).

from wild-type (or EGFP-expressing) SCG cells, the phasic, adapting, and tonic firing patterns were also observed in SCG neurons expressing Kv4.2W362F. In contrast to control cells, however, the majority (52%) of Kv4.2W362F-expressing cells are adapting (Fig. 7*B*). This increase in the number of adapting cells reflects a decline in the fraction of neurons displaying the phasic phenotype from 43% of wild-type neurons (Fig. 6*B*, Table 2) to 24% of Kv4.2W362F-expressing cells (Fig. 7*B*, Table 3). The percentage of tonic cells, in contrast, is unaffected by loss of I_{Af}: ~25% of wild-type (Fig. 6*C*, Table 2) and Kv4.2W362F-expressing (Fig. 7*C*, Table 3) cells fire tonically. These observations suggest that low I_{Af} density correlates with the adapting phenotype (see Discussion). In addition to the redistribution of cells, the input resistances of phasic and tonic cells expressing Kv4.2W362F (Table 3) are significantly ($p < 0.001$) higher than in wild-type (phasic and tonic) cells (Table 2), whereas the input resistances in adapting cells expressing Kv4.2W362F were not significantly different from wild-type adapting cells (Table 2). Indeed, the input resistances of Kv4.2W362F-expressing phasic, adapting, and tonic SCG cells are similar (Table 3). Consistent with this increase in input resistance, the current thresholds for firing single action potentials (and trains) in Kv4.2W362F-expressing phasic and tonic cells are significantly ($p < 0.003$) lower (Table 3) than in wild-type (phasic and tonic) cells (Table 2).

In contrast to the marked effects on excitability, action potential durations are not affected measurably by elimination of I_{Af} (Table 3). These observations suggest that I_{Af} does not play a prominent role in determining action potential durations in SCG neurons (see Discussion). Tonic cells expressing Kv4.2W362F, however, fire at higher frequencies (Fig. 7) than their wild-type counterparts (Fig. 6) in response to current injections of the same amplitude. In response to a 200 pA current injection, for example, wild-type tonic

Table 3. Expression of Kv4.2W362F increases input resistance and the number of adapting SCG neurons[a]

Phenotype	R_{in} (GΩ)	V_m (mV)	AP$_{Thresh}$ (pA)	APA (mV)	APD$_{50}$ (msec)	APD$_{90}$ (msec)	n
All cells	68 ± 0.08	−49 ± 1	28 ± 2	90 ± 2	3.54 ± 0.27	5.59 ± 0.22	25
Phasic	0.64 ± 0.14*	−47 ± 2	30 ± 7**	82 ± 3	3.63 ± 0.44	6.07 ± 0.33	6
Adapting	0.76 ± 0.12	−47 ± 1	26 ± 3	89 ± 2	3.47 ± 0.14	5.76 ± 0.23	13
Tonic	0.60 ± 0.09**	−53 ± 3	27 ± 2*	99 ± 4	2.90 ± 0.09	4.90 ± 0.20[+]	6

*,**Values are significantly different from those in wild-type cells at the $p < 0.003$* and $p < 0.001$** levels. [+]Values are significantly different from those in phasic or adapting cells at the $p < 0.01$ level.
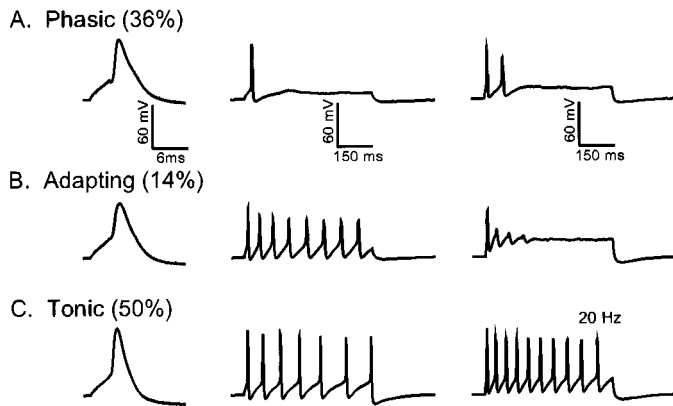
[a]All values are means ± SEM.

Figure 8. Increased I_{Af} density decreases action potential durations and increases the percentage of tonic SCG neurons. Action potentials and repetitive firing patterns, recorded as described in the legend to Figure 6, were obtained from isolated SCG neurons 24 hr after transfection with wild-type Kv4.2. Records from three representative cells are shown in *A–C*. As in wild-type cells, the phasic (*A*), adapting (*B*), and tonic (*C*) firing patterns were seen in Kv4.2 overexpressing cells. In cultures overexpressing Kv4.2, however, the percentage of adapting cells is lower and the percentage of tonic cells is higher than seen in wild-type (Table 2) or Kv4.2W362F-expressing (Table 3) SCG cells.

cells fire at mean ± SEM frequencies of 15 ± 1 Hz, whereas Kv4.2W362F-expressing cells fire at 29 ± 2 Hz. The likely interpretation of this observation is the fact that the current thresholds for action potential generation are decreased in cells expressing Kv4.2W362F (Table 3) as compared with wild-type cells (Table 2).

Increasing I_{Af} reduces the number of adapting cells

The results of the experiments above suggest that low I_{Af} density is an important determinant of the adapting phenotype. To further test this hypothesis, the effects of increasing I_{Af} density on the firing properties of SCG neurons were examined. In these experiments, SCG neurons were transfected with a construct encoding wild-type Kv4.2 (as well as EGFP), and current-clamp recordings were obtained from EGFP-positive cells. These experiments revealed firing patterns (Fig. 8) that are indistinguishable from those of wild-type (and EGFP-expressing) SCG neurons (Fig. 6), although the distribution of cells displaying the various firing patterns is quite distinct (Table 4). Half of the cells transfected with the Kv4.2 construct are tonic (Fig. 8*C*), only 14% of the cells are adapting (Fig. 8*B*), and the remaining 36% of the cells are phasic (Fig. 8*A*). There is a marked increase in tonic cells and a corresponding decrease in the number of adapting cells with overexpression of Kv4.2 (Fig. 8*B*, Table 4). The properties of the Kv4.2-expressing cells that are adapting (Fig. 8*B*) are also distinct from those of wild-type adapting cells (Table 2) in that the current threshold for action potential generation is increased significantly ($p < 0.003$) by Kv4.2 expression (Table 4), consistent with a decrease in input resistance (Table 4). These results suggest that all adapting cells are converted to phasic or tonic cells as a function of I_{Af} density (see Discussion). Analysis of the waveforms of evoked action potentials also revealed that APD$_{50}$ values (Table 4) in Kv4.2-expressing phasic cells are significantly ($p < 0.001$) shorter

than in wild-type phasic cells (Table 2). In contrast, mean action potential durations in adapting and tonic SCG cells overexpressing Kv4.2 are not significantly different from those in wild-type (adapting and tonic) SCG cells (compare Table 2 and Table 4).

Analysis of voltage-clamp recordings from EGFP-positive cells in Kv4.2-transfected cultures revealed that the density of I_{Af} is increased relative to the currents in wild-type (and EGFP-expressing) SCG neurons. In all cells expressing wild-type Kv4.2, a prominent fast transient current is evident (Fig. 9). Analysis of the decay phases of the outward currents revealed that inactivation is best described by the sum of two (Fig. 9*A*) or three (Fig. 9*B*) exponentials. The mean ± SEM decay time constants derived from these fits are similar to those determined in wild-type I and II SCG cells (Table 1). No Type III neurons, which lack I_{Af} and I_{As} (Table 1), were seen among the cells expressing Kv4.2. In the majority (69%) of the cells overexpressing Kv4.2, I_{Af}, I_K, and I_{SS} are detected (Table 1). The waveforms of the currents (Fig. 9*A*) are similar to those in wild-type I cells (Fig. 3*A*), although I_{Af} density is significantly ($p < 0.04$) higher and I_K and I_{SS} densities are significantly ($p < 0.005$) lower than in wild-type Type I cells (Table 1). In the remaining Kv4.2-expressing cells, three exponentials were required to fit the decay phases of the outward currents. These cells (Fig. 9*B*) are similar to wild-type Type II cells, expressing I_{Af}, I_{As}, I_K, and I_{SS}, although I_{Af} density is significantly ($p < 0.04$) higher in the Kv4.2-expressing cells (Table 1).

DISCUSSION

Kv4 α-subunits underlie I_{Af} in SCG neurons

In the experiments here, four kinetically distinct voltage-gated K$^+$ currents have been distinguished in SCG neurons: two transient currents, I_{Af} and I_{As}, as well as a slowly inactivating current, I_K, and a steady-state current, I_{SS} (Table 1). In addition, these currents are differentially distributed, and SCG cells have been classified as Type I, II, or III based on expression differences. Type I cells express I_{Af}, I_K, and I_{SS}, whereas Type II cells express I_{Af}, I_{As}, I_K, and I_{SS}, and Type III cells express only I_K and I_{SS}. There is considerable variability in current densities within each grouping (Table 1), and interestingly, I_K and I_{SS} densities are significantly ($p < 0.005$) lower in Type II cells (the only cells that express I_{As}) than in either Type I or III cells (Table 1).

In experiments aimed at testing the hypothesis that α-subunits of the Kv4 subfamily of voltage-gated K$^+$ channels underlie I_{Af} in SCG neurons, the biolistics method (gene gun) was used to introduce a mutant Kv4.2 α-subunit, Kv4.2W362F, that functions as a dominant negative (Barry et al., 1998), into these cells *in vitro*. Voltage-clamp recordings from Kv4.2W362F-expressing cells revealed that in the vast majority (~80%) of cells no fast transient outward currents (I_{Af}) were detected (Fig. 3, Table 1). The densities of the other currents, I_{As}, I_K, and I_{SS}, are largely unaffected by Kv4.2W362F expression, although I_K density is significantly higher in the I_{As}-expressing subset of these cells (Table 1, column B) than in wild-type Type II cells (Table 1). The simplest interpretation of these findings is that I_{Af} is encoded by Kv4 α-subunits in most SCG neurons. Consistent with this hypothesis, I_{Af} was evident in all cells expressing wild-type Kv4.2 (Fig. 9), and mean I_{Af} density was significantly ($p < 0.04$) higher than in wild-type cells (Table 1).

Nevertheless, a rapidly inactivating current remains in ~20% (6

Table 4. Overexpression of Kv4.2 reduces the input resistance and the number of adapting neurons[a]

Phenotype	R_{in} (GΩ)	V_m (mV)	AP_{Thresh} (pA)	APA (mV)	APD_{50} (msec)	APD_{90} (msec)	n
All cells	0.35 ± 0.05	-52 ± 1	43 ± 4	92 ± 2	2.78 ± 0.10	4.87 ± 0.17	28
Phasic	0.23 ± 0.03	-52 ± 1	58 ± 9	89 ± 3	2.87 ± 0.15**	5.05 ± 0.25*	10
Adapting	0.46 ± 0.07[+]	-51 ± 2	39 ± 4*	86 ± 2	3.03 ± 0.20	5.28 ± 0.24	4
Tonic	0.29 ± 0.04	-51 ± 1	45 ± 4	95 ± 2	2.70 ± 0.19	4.75 ± 0.24	14

*,**Values are significantly different from those in wild-type cells at the $p < 0.003$* and $p < 0.001$** levels. [+]Values are significantly ($p < 0.005$) different from those in phasic cells.

[a]All values are means $\pm$ SEM.

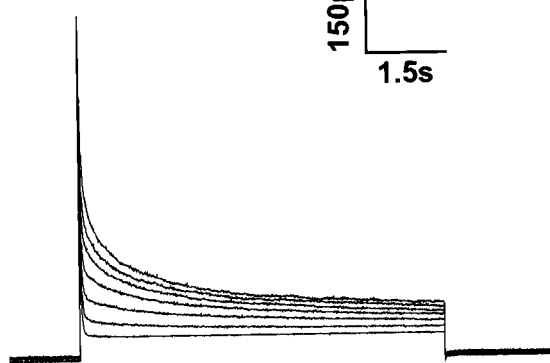## A. Type I
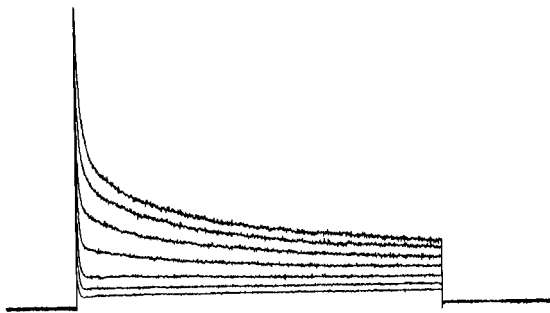
B. Type II

Figure 9. Overexpression of Kv4.2 increases I_{Af} density in SCG neurons. Isolated SCG neurons were transfected with Kv4.2 (and EGFP), and outward K^{+} currents were recorded from EGFP-expressing cells as described in the legend to Figure 1. Records similar to those in *A* and *B* were obtained from all cells (Table 1); no cells lacking I_{Af} were evident. Analysis of the decay phases of the currents provided the mean $\pm$ SEM densities of I_{Af}, I_{As}, I_K, and I_{SS} (Table 1), and mean $\pm$ SEM I_{Af} densities were increased significantly in both Type I (*A*) and Type II (*B*) SCG cells as compared with wild-type Type I and II cells (Table 1).

of 31) of the SCG cells expressing Kv4.2W362F (Table 1). The density of this fast transient current is somewhat lower than I_{Af} density in wild-type Type I or II cells (Table 1), which could reflect incomplete removal of Kv4-induced currents. Alternatively, it is possible that there are two populations of I_{Af} channels, one generated by Kv4 α-subunits and the other by another Kv subfamily. Analysis of the decay phases of the currents revealed that τ_{decay} values for I_{Af} in wild-type Type I and II cells are quite variable, ranging from 53 to 209 msec, and that there appear to be two populations of cells (Fig. 5). In cells expressing Kv4.2W362F, in contrast, the τ_{decay} for the rapid component of current decay ranged from 139 to 254 msec; there were no cells with τ_{decay} values in the 50–130 msec range (Fig. 5). In Kv4.2-expressing SCG cells, the τ_{decay} values for I_{Af} are all < 130 msec (Fig. 5). Because the mean $\pm$ SEM τ_{decay} values for I_{Af} recorded from Kv4.2- and Kv4.2W362F-

expressing cells are significantly different ($p < 0.001$) and the distribution of τ values is nonoverlapping (Fig. 5), it seems reasonable to suggest that there are two distinct types of I_{Af} channels in SCG neurons that reflect the functional expression of distinct gene products. Interestingly, the identification of two molecularly distinct components of a "single" electrophysiologically defined current has been reported previously for I_{Kr} in *Xenopus* spinal neurons (Ribera, 1996) and for $I_{K, slow}$ in mouse ventricular myocytes (Xu et al., 1999b). Recent studies have also revealed two components of recovery of I_{Af} from steady-state inactivation with time constants of ~100 and ~1000 msec ($n = 2$), observations consistent with the suggestion that there are two components I_{Af}. The more rapidly inactivating currents (mean $\tau_{decay} \sim 80$ msec) present in the majority (80%) of (Type I and II) SCG neurons reflect the expression of Kv4 α-subunits. Although the molecular identity of the fast transient current I_{Af} remaining in (~20%) Kv4.2W362F-expressing cells has not been defined, one potential candidate is Kv1.4, a Kv α-subunit that also produces A-type K^{+} currents when expressed in heterologous systems (Rudy, 1988). Importantly, Kv1.4 mRNA expression has been documented in SCG neurons (Dixon and McKinnon, 1996). Further experiments aimed at testing directly the hypothesis that Kv1.4 underlies the more slowly inactivating component of I_{Af} are clearly warranted.

I_{Af} density and neuronal excitability

Whole-cell current-clamp recordings from SCG neurons revealed distinct repetitive firing patterns, and cells were classified as phasic, adapting, or tonic based on stereotyped differences in the response to prolonged current injections (Fig. 6). The waveforms of individual action potentials recorded in phasic, tonic, and adapting cells are similar (Fig. 6), although action potential durations are briefer in tonic than in phasic or adapting cells (Table 2). There are also significant differences in the input resistances and current thresholds for action potential generation in adapting compared with phasic or tonic cells (Table 2). In SCG cells expressing Kv4.2W362F, the mean $\pm$ SEM input resistances were increased compared with wild-type cells (Table 3). This finding suggests that (some) I_{Af} channels are open at rest, an observation supported by voltage-clamp data documenting an "window current" in the -70 to -50 mV range (Belluzzi et al., 1985a). Preliminary experiments have revealed that perfusion of wild-type SCG neurons with 300 nm Heteropoda toxin-3 (HpTx), a spider toxin (Sanguinetti et al., 1997) that blocks I_{Af} selectively ($n = 2$), increases the input resistances of SCG neurons to a mean $\pm$ SEM of 0.74 ± 0.27 GΩ ($n = 17$) from the control values of 0.45 ± 0.11 GΩ ($n = 16$). Importantly, neither the expression of Kv4.2W362F nor the application of HpTx-3 affects I_{K1} density. Thus, the removal of I_{Af} specifically increases input resistance. The concomitant decrease in the current threshold for action potential generation (compare Table 2 and Table 3) reveals that I_{Af} regulates excitability in SCG neurons by opposing depolarizing inputs and influencing the current required to reach threshold.

The results presented here also reveal that elimination of I_{Af} (by Kv4.2W362F expression) does not measurably affect action potential duration in SCG neurons. This finding seems in conflict with several previous studies suggesting that I_{Af} (I_A) plays a role in action potential repolarization in SCG cells. Action potential durations, for example, reportedly decrease during late embryonic development in parallel with an increase in I_{Af} density (Nerbonne

and Gurney, 1989). In addition, in SCG neurons, action potential durations follow the steady-state inactivation curve for I_{Af} and are prolonged by 4-AP (Belluzzi et al., 1985a). These seemingly disparate findings could reflect the fact that additional currents (to I_A) are changing during development and/or are affected by 4-AP. The molecular genetic approach to manipulating functional K$^+$ channel expression used here, however, should not be confounded by these uncertainties. Importantly, action potential durations are decreased when Kv4.2 is overexpressed and I_{Af} is increased.

The role of I_{Af} in determination of firing patterns

The experiments completed here reveal that I_{Af} does play a prominent role in determining the repetitive firing properties of SCG neurons. Elimination of I_{Af} resulted in an increase in the input resistances of phasic and tonic (but not adapting) cells (Table 3). The loss of I_{Af} also resulted in an increased number (and percentage) of adapting cells (Table 3), whereas increasing the density of I_{Af} decreased the number of adapting cells (Table 4). Taken together, these results suggest that low I_{Af} density is correlated with the adapting firing pattern. The changes in the distributions of cells also suggest that reductions in I_{Af} density can convert phasic cells to the adapting phenotype. Adapting cells, in contrast, can be made to fire tonically when I_{Af} density is increased. Thus, although I_{Af} is not the sole determinant of repetitive firing patterns in SCG neurons, this conductance does play a prominent role.

Tonic cells are characterized by briefer action potentials than phasic or adapting cells (Table 2), and shortening action potential duration by increasing I_{Af} expression increases the percentage of tonic cells (Table 4). Nevertheless, ~30% of Kv4.2-expressing cells are phasic (Table 4), suggesting that currents other than I_{Af} play an important role in defining this firing class. One likely candidate is the M-current, I_M, which has been linked previously to phasic firing in SCG and other neurons (Brown and Adams, 1980; Freshi, 1983; Galvan and Sedlmeir, 1984; Cassell et al., 1986; Wang and McKinnon, 1995). Blockade of the M-current has previously been shown to be sufficient to convert phasic SCG neurons to tonic firing (Cassell et al., 1986). Interestingly, the results here show that the same conversion may be accomplished with a decrease in action potential duration, which suggests that action potential duration is a key component of I_M activation and regulation of repetitive firing properties in SCG neurons. Further experiments aimed at testing this hypothesis directly are clearly warranted.

REFERENCES

Baro DJ, Levini RM, Kim MT, Willms AR, Lanning CC, Rodriguez HE, Harris-Warrick RM (1997) Quantitative single-cell-reverse transcription-PCR demonstrates that A-current magnitude varies as a linear function of *shal* gene expression in identified stomatogastric neurons. J Neurosci 17:6597–6610.

Barry DM, Trimmer JS, Merlie JP, Nerbonne JM (1995) Differential expression of voltage-gated K$^+$ channel subunits in adult rat heart. Relation to functional K$^+$ channels? Circ Res 77:361–369.

Barry DM, Xu H, Schuessler RB, Nerbonne JM (1998) Functional knockout of the transient outward current, long-QT syndrome, and cardiac remodeling in mice expressing a dominant-negative Kv4 α-subunit. Circ Res 83:560–567.

Belluzzi O, Sacchi O, Wanke E (1985a) Identification of delayed potassium and calcium currents in the rat sympathetic neurone under voltage clamp. J Physiol (Lond) 358:109–129.

Belluzzi O, Sacchi O, Wanke E (1985b) A fast transient outward current in the rat sympathetic neurone studied under voltage-clamp conditions. J Physiol (Lond) 358:91–109.

Brahmajothi MV, Campbell DL, Rasmusson RL, Morales MJ, Trimmer JS, Nerbonne JM, Strauss HC (1999) Distinct transient outward potassium current (I_{to}) phenotypes and distribution of fast-inactivating potassium channel alpha subunits in ferret left ventricular myocytes. J Gen Physiol 113:581–600.

Brown DA, Adams PR (1980) Muscarinic suppression of a novel voltage-sensitive K$^+$ current in a vertebrate neurone. Nature 283:673–676.

Cassell JF, Clark AL, McLachlan EM (1986) Characteristics of phasic and tonic sympathetic ganglion cells of the guinea-pig. J Physiol (Lond) 372:457–483.

Chang JY, Martin DP, Johnson EM Jr (1990) Interferon suppresses sympathetic neuronal cell death caused by nerve growth factor deprivation. J Neurochem 55:436–445.

Coetzee WA, Amarillo Y, Chiu J, Chow A, Lau D, McCormack T, Moreno H, Nadal MS, Ozaita A, Pountney D, Saganich M, Vega-Saenz de Meira E, Rudy B (1999) Molecular diversity of K$^+$ channels. Ann NY Aca Sci 868:233–285.

Dixon JE, McKinnon D (1996) Potassium channel mRNA expression in prevertebral and paravertebral sympathetic neurons. Eur J Neurosci 8:183–191.

Fiset C, Clark RB, Larsen T, Giles WR (1997) A rapidly activating sustained current modulates repolarization and excitation-contraction coupling in adult mouse ventricle. J Physiol (Lond) 504:557–563.

Freshi JE (1983) Membrane currents of cultured rat sympathetic neurons under voltage clamp. J Neurophysiol 50:1460–1478.

Galvan M, Sedlmeir C (1984) Outward currents in voltage-clamped rat sympathetic neurones. J Physiol (Lond) 356:115–133.

Johns DC, Nuss HB, Marban E (1997) Suppression of neuronal and cardiac transient outward currents by viral gene transfer of dominant-negative Kv4.2 constructs. J Biol Chem 272:31598–31603.

Martina M, Schultz JH, Ehmke H, Monyer H, Jonas P (1998) Functional and molecular differences between voltage-gated K$^+$ channels of fast-spiking interneurons and pyramidal neurons of the hippocampus. J Neurosci 18:8111–8125.

McFarlane S, Cooper E (1992) Postnatal development of voltage-gated K$^+$ currents on rat sympathetic neurons. J Neurophysiol 67:1291–1300.

Nerbonne JM, Gurney AM (1989) Development of excitable properties in mammalian sympathetic neurons. J Neurosci 9:3272–3286.

Nerbonne JM, Gurney AM, Rayburn H (1986) Development of the fast, transient outward K$^+$ current in embryonic sympathetic neurones. Brain Res 378:197–202.

Pankevych H, Kristufek D, Huck S (1999) Perinatal and postnatal regulation of Shaker-related genes in rat superior cervical ganglion. Soc Neurosci Abstr 29:789.

Pond AL, Scheve BK, Benedict AB, Petrecca K, Van Wagoner DR, Schrier A, Nerbonne JM (2000) Expression of distinct ERG proteins in rat, mouse and human heart. J Biol Chem 275:5997–6006.

Pongs O (1999) Voltage-gated potassium channels: from hyperexcitability to excitement. FEBS Lett 452:31–35.

Raff MC, Fields KL, Hakomori S-I, Mirsky R, Pruss RM, Winter J (1979) Cell-type-specific markers for distinguishing and studying neurons and the major classes of glial cells in culture. Brain Res 174:283–308.

Ribera AB (1996) Homogeneous development of electrical excitability via heterogeneous ion channel expression. J Neurosci 16:1123–1130.

Rudy B (1988) Diversity and ubiquity of K channels. Neuroscience 24:729–749.

Sanguinetti MC, Johnson JH, Hammerland LG, Kelbaugh PR, Volkmann RA, Saccomano NA, Mueller AL (1997) Heteropodatoxins: peptides isolated from spider venom that block Kv4.2 potassium channels. Mol Pharmacol 51:491–498.

Serodio P, Kentros C, Rudy B (1994) Identification of molecular components of A-type channels activating at subthreshold potentials. J Neurophysiol 72:1516–1529.

Song W-J, Tkatch T, Baranauskas G, Ichinohe N, Kitai ST, Surmeier DJ (1998) Somatodendritic depolarization-activated potassium currents in rat neostriatal cholinergic interneurons are predominantly of the A type and attributable to coexpression of Kv4.2 and Kv4.1 subunits. J Neurosci 18:3124–3137.

Storm JF (1990) Potassium currents in hippocampal pyramidal cells. Prog Brain Res 83:161–187.

Tkatch T, Baranauskas G, Surmeier DJ (2000) Kv4.2 mRNA abundance and A-type K$^+$ current amplitude are linearly related in basal ganglia and basal forebrain neurons. J Neurosci 20:579–588.

Wang H-S, McKinnon D (1995) Potassium currents in rat prevertebral and paravertebral sympathetic neurones: control of firing properties. J Physiol (Lond) 485:319–335.

Xu H, Li H, Nerbonne JM (1999a) Elimination of the transient outward current and action potential prolongation in mouse atrial myocytes expressing a dominant negative Kv4 α-subunit. J Physiol (Lond) 519:11–21.

Xu H, Barry DM, Li H, Brunet S, Guo W, Nerbonne JM (1999b) Attenuation of the slow component of delayed rectification, action potential prolongation, and triggered activity in mice expressing a dominant-negative Kv2 α-subunit. Circ Res 85:623–633.